

## Atom Interferometry with Bose-Einstein Condensates in a Double-Well Potential

Y. Shin, M. Saba, T. A. Pasquini, W. Ketterle, D. E. Pritchard, and A. E. Leanhardt\*

*Department of Physics, MIT-Harvard Center for Ultracold Atoms, and Research Laboratory of Electronics, Massachusetts Institute of Technology, Cambridge, Massachusetts 02139, USA*

(Received 17 July 2003; published 6 February 2004)

A trapped-atom interferometer was demonstrated using gaseous Bose-Einstein condensates coherently split by deforming an optical single-well potential into a double-well potential. The relative phase between the two condensates was determined from the spatial phase of the matter wave interference pattern formed upon releasing the condensates from the separated potential wells. Coherent phase evolution was observed for condensates held separated by  $13\ \mu\text{m}$  for up to 5 ms and was controlled by applying ac Stark shift potentials to either of the two separated condensates.

DOI: 10.1103/PhysRevLett.92.050405

PACS numbers: 03.75.Dg, 03.75.Lm, 39.20.+q

Atom interferometers have been used to sense accelerations [1,2] and rotations [3,4], monitor quantum decoherence [5], characterize atomic and molecular properties [6], and measure fundamental constants [1,7]. Demonstrating atom interferometry with particles confined by magnetic [8–11] and optical [12] microtraps and waveguides would realize the matter wave analog of optical interferometry using fiber-optic devices. Current proposals for confined-atom interferometers rely on the separation and merger of two potential wells to split and recombine atomic wave packets [13–15]. Atom-atom interactions tend to localize particles in either potential well and reduce the coherence of the splitting and recombination processes [16,17], whereas tunneling serves to delocalize the atomic wave packets and maintain a well-defined relative phase between the potential wells [16].

Bose-Einstein condensates are to matter wave interferometry what lasers are to optical interferometry, i.e., a coherent, single-mode, and highly brilliant source. Condensates have been coherently delocalized over multiple sites in optical lattices where the tunneling energy dominates the on-site atom-atom interaction energy due to the submicron barrier between neighboring potential wells [2,18–21]. Here, the thin barrier helps to maintain phase coherence across the lattice, but also prevents addressing individual lattice sites. To construct a versatile atom interferometer capable of sensing forces with arbitrary spatial variation two individually addressable interfering paths are needed. This apparently simple requirement represents a considerable challenge when it comes to splitting a Bose-Einstein condensate with a thick barrier that prevents tunneling and separates the resulting condensate pair by large distances (that allow for individual addressability) without affecting their quantum mechanical phase in an uncontrolled way. In addition to the technical challenges, it is not even clear theoretically if the two condensates generated after splitting will share the same phase (a phase-coherent state) or if each will have a well-defined number of particles without relative phase coherence (a number-squeezed state) [16,22–24].

In this Letter, we demonstrate that a condensate can be split coherently along two separated paths by deforming an initially single-well potential into two wells. The relative phase between the two condensates was determined from the spatial phase of the matter wave interference pattern formed upon releasing the atoms from the separated potential wells [25,26]. This scheme realizes a trapped-atom interferometer. The large well separation ( $13\ \mu\text{m}$ ) (i) allowed ac Stark phase shifts to be applied to either condensate by temporarily turning off the laser beam generating its potential well and (ii) suppressed tunneling such that the phase of each condensate evolved independently. Without the aid of tunneling to preserve phase coherence, the measured coherence time of the separated condensates was 5 ms.

Bose-Einstein condensates containing over  $10^7$   $^{23}\text{Na}$  atoms were created in the  $|F = 1, m_F = -1\rangle$  state in a magnetic trap, captured in the focus of a 1064 nm optical tweezers laser beam, and transferred into an auxiliary “science” chamber as described in Ref. [27]. In the science chamber, the condensate was loaded from the optical tweezers into a secondary optical trap formed by a counterpropagating, orthogonally polarized 1064 nm laser beam. The secondary optical trap was formed by a collimated laser beam that passed through an acousto-optic modulator (AOM) and was focused onto the condensate with a lens [Fig. 1(a)]. The AOM was driven simultaneously by two radio frequency (rf) signals to tailor the shape of the potential from single well [Fig. 1(b)] to double well [Fig. 1(c)]. The separation between the potential wells was controlled by the frequency difference between the rf drives. The waist of each focused beam was  $5\ \mu\text{m}$ . A single, isolated potential well was characterized by a trap depth  $U_0 = h \times 5\ \text{kHz}$ , where  $h$  is Planck’s constant, and a radial (axial) trap frequency  $f_r = 615\ \text{Hz}$  ( $f_z = 30\ \text{Hz}$ ).

Condensates were initially loaded from the tweezers into a single-well trap [Fig. 1(b)]. After holding the cloud for 15 s to damp excitations, the condensate contained  $\sim 10^5$  atoms with a peak atomic mean field energy

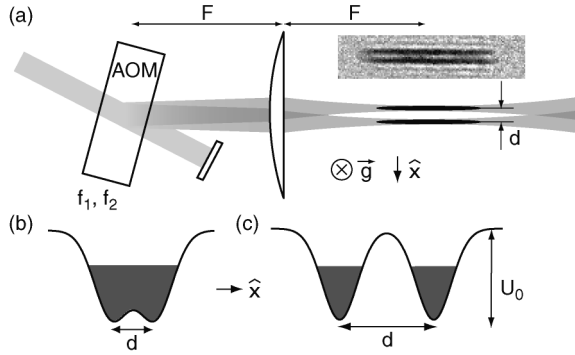


FIG. 1. Optical double-well potential. (a) Schematic diagram of the optical setup for the double-well potential. An acousto-optic modulator (AOM) was driven by two frequencies,  $f_1$  and  $f_2$ , and diffracted a collimated beam into two beams. The AOM was placed in the focal plane of a lens of focal length  $F$  so that the two beams propagated parallel to each other. The radial separation of the potential wells,  $d$ , was controlled by the frequency difference,  $\Delta f = |f_1 - f_2|$ . The acceleration due to gravity,  $\vec{g}$ , points into the page. The absorption image shows two well-separated condensates confined in the double-well potential diagrammed in (c). The field of view is  $70 \times 300 \mu\text{m}$ . Energy diagrams for (b) initial single-well trap with  $d = 6 \mu\text{m}$  and (c) final double-well trap with  $d = 13 \mu\text{m}$ . In both (b) and (c),  $U_0 = \hbar \times 5 \text{ kHz}$  and the peak atomic mean field energy was  $\sim \hbar \times 3 \text{ kHz}$ . The potential “dimple” in (b) was  $< \hbar \times 500 \text{ Hz}$  which was much less than the peak atomic mean field energy allowing the trap to be characterized as a single well. The potential “barrier” in (c) was  $\hbar \times 4.7 \text{ kHz}$  which was larger than the peak atomic mean field energy allowing the resulting split condensates to be characterized as independent.

$\mu \approx \hbar \times 3 \text{ kHz}$ . The single-well trap was deformed into a double-well potential [Fig. 1(c)] by linearly increasing the frequency difference between the rf signals driving the AOM over 5 ms. The amplitudes of the rf signals were tailored during the splitting process to yield nearly equal atom number and trap depths for each potential well.

Condensates realized from the double-well potential ballistically expanded, overlapped, and interfered (Fig. 2). Each realization of the experiment produced a matter wave interference pattern with the same spatial phase. This reproducibility demonstrated that deforming the optical potential from a single well into a double well coherently split the condensate into two clouds with deterministic relative phase, i.e., the relative phase between the two condensates was the same from shot to shot.

This experiment derived its double-well potential from a single laser beam passing through an AOM. Vibrations and fluctuations of the laser beam were common mode to both wells, and a clean and rapid trap turn-off was achieved by switching off the rf power driving the AOM. In contrast, past experiments created a double-well potential by splitting a magnetically trapped condensate with a blue-detuned laser beam [25]. Such work was unable to observe a reproducible relative phase be-

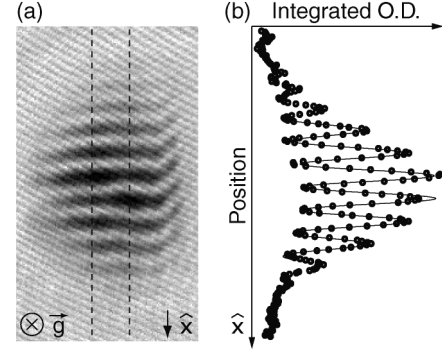


FIG. 2. Matter wave interference. (a) Absorption image of condensates released from the double-well potential in Fig. 1(c) immediately after splitting and allowed to overlap during 30 ms of ballistic expansion. The imaging axis was parallel to the direction of gravitational acceleration,  $\vec{g}$ . The field of view is  $600 \times 350 \mu\text{m}$ . (b) Radial density profiles were obtained by integrating the absorption signal between the dashed lines, and typical images gave  $> 60\%$  contrast. The solid line is a fit to a sinusoidally modulated Gaussian curve from which the phase of the interference pattern was extracted (see text). This figure presents data acquired in a single realization of the experiment.

tween the split condensates, due to fluctuations in the blue-detuned laser beam and irreproducible turn-off of the high current magnetic trap that initiated ballistic expansion.

The relative phase between the two separated condensates was determined by the spatial phase of their matter wave interference pattern. For a ballistic expansion time  $t \gg 1/f_r$ , each condensate had a quadratic phase profile [28],  $\psi_{\pm}(\vec{r}, t) = \sqrt{n_{\pm}(\vec{r}, t)} \exp[i(m/2\hbar t)|\vec{r} \pm \vec{d}/2|^2 + \phi_{\pm}]$ , where  $\pm$  denotes either well,  $n_{\pm}$  is the condensate density,  $m$  is the atomic mass,  $\vec{d}$  is a vector connecting the two wells,  $\phi_{\pm}$  is the condensate phase, and  $\hbar = \hbar/2\pi$ . Interactions between the two condensates during ballistic expansion have been neglected. The total density profile for the matter wave interference pattern takes the form

$$n(\vec{r}, t) = \left[ n_+ + n_- + 2\sqrt{n_+ n_-} \cos\left(\frac{m\vec{d}}{\hbar t} \cdot \vec{r} + \phi_r \right) \right], \quad (1)$$

where  $\phi_r = \phi_+ - \phi_-$  is the relative phase between the two condensates and  $\vec{d} = d\hat{x}$ . To extract  $\phi_r$ , an integrated cross section of the matter wave interference pattern [Fig. 2(b)] was fitted with a sinusoidally modulated Gaussian curve,  $G(x) = A \exp[-(x - x_c)^2/\sigma^2] \{1 + B \cos[(2\pi/\lambda)(x - x_0) + \phi_f]\}$ , where  $\phi_f$  is the phase of the interference pattern with respect to a chosen fixed  $x_0$ . Ideally, if  $x_0$  was set at the center of the two wells, then  $\phi_r = \phi_f$ . However, misalignment of the imaging axis with the direction of gravitational acceleration created a constant offset,  $\phi_f = \phi_r + \delta\phi$ . With  $t = 30 \text{ ms}$  the measured fringe period,  $\lambda = 41.5 \mu\text{m}$ , was within 4% of the point source formula prediction [Eq. (1)],  $\hbar t/md = 39.8 \mu\text{m}$ .

The relative phase between the separated condensates was observed to evolve linearly in time [Fig. 3(a)]. This evolution was primarily due to a small difference in the well depths and could be tailored by adjusting the relative intensity of the two laser beams generating the wells.

The standard deviation of eight measurements of  $\phi_r$  was  $<90^\circ$  for condensates split then held separated for  $\leq 5$  ms [Fig. 3(b)]. For hold times  $\leq 1$  ms, the standard deviation was substantially smaller,  $<40^\circ$ . Since a random distribution of phases between  $-180^\circ$  and  $+180^\circ$  would have a standard deviation of  $\sim 104^\circ$ , the measured results quantitatively confirm the reproducible nature of the splitting process and the coherent evolution of the separated condensates.

The number-phase uncertainty principle provides a fundamental limit to the phase coherence between isolated condensates due to phase diffusion [16,22–24,29,30]. For Poissonian number fluctuations about a mean condensate atom number  $N$ , we expect a phase diffusion time  $\sim 1/(2\mu/5h\sqrt{N}) \sim 250$  ms. Atom-atom interactions may localize particles in either potential well during splitting and reduce the relative number fluctuations. This would reduce the measured coherence of the split condensates, but extend the phase diffusion time. The uncertainty in determining  $\phi_r$  at hold times  $> 5$  ms is attributed to axial and breathing-mode excitations created during the splitting process. These excitations led to interference fringes that were angled and had

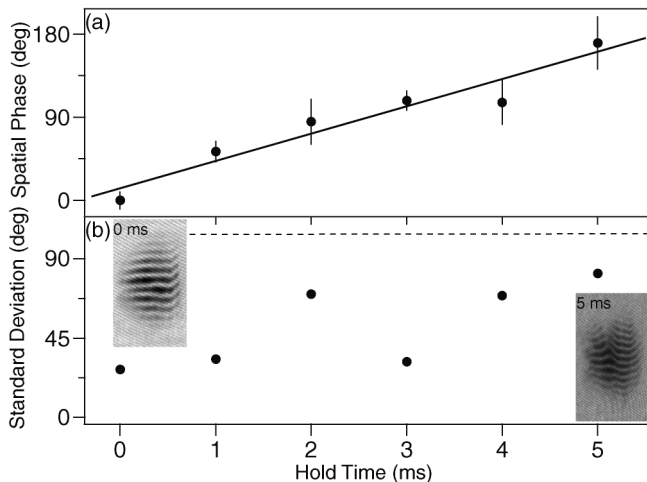


FIG. 3. Phase coherence of the separated condensates. (a) The spatial phase of the matter wave interference pattern is plotted versus hold time after splitting the condensate. Each point represents the average of eight measurements. The phase evolution was due to unequal trap depths for the two wells, which was determined from the linear fit to be  $h \times 70$  Hz or  $\sim 1\%$  of the trap depth. (b) Standard deviation of eight measurements of the relative phase. A standard deviation  $\sim 104^\circ$  (dashed line) is expected for random relative phases. Matter wave interference patterns after 0 and 5 ms holding are displayed. The curvature of the interference fringes increased with hold time limiting the coherence time of the separated condensates to 5 ms.

050405-3

substantial curvature, rendering a determination of  $\phi_r$  impossible. Splitting the condensate more slowly did not improve the measured stability of  $\phi_r$  since we were unable to split the condensate much slower than the axial trap period and much faster than the expected phase diffusion time.

The phase sensitivity of the trapped-atom interferometer was demonstrated by applying ac Stark phase shifts to either (or both) of the two separated condensates. Phase shifts were applied to individual condensates by pulsing off the optical power generating the corresponding potential well for a duration  $\tau_p \ll 1/f_r$ . The spatial phase of the matter wave interference pattern shifted linearly with the pulse duration, as expected [Fig. 4(a)]. Because of the inhomogeneous optical potential,  $U(r)$ , the applied ac Stark phase shifts varied across the condensate as  $\Delta\phi(r) = -U(r)\tau_p/\hbar$ . Inhomogeneous phase shifts should lead to an excitation of the condensate that was

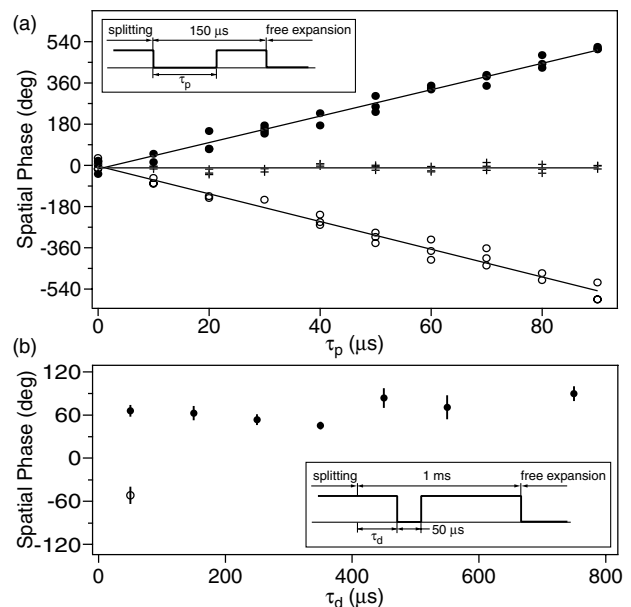


FIG. 4. Trapped-atom interferometry. (a) ac Stark phase shifts were applied to either well exclusively (solid circles and open circles) or both wells simultaneously (crosses) by turning off the corresponding rf signal(s) driving the AOM for a duration  $\tau_p$ . The resulting spatial phase of the matter wave interference pattern scaled linearly with  $\tau_p$  and hence the applied phase shift. Applying the ac Stark shift to the opposite well (solid versus open circles) resulted in an interference pattern phase shift with opposite sign. Applying ac Stark shifts to both wells (crosses) resulted in no phase shift for the interference pattern. These data were taken with a slightly modified experimental setup such that the trap depth of the individual potential wells was  $U_0 = h \times 17$  kHz, corresponding to a  $270^\circ$  phase shift for a  $50 \mu\text{s}$  pulse. (b) A  $50 \mu\text{s}$  pulse induced a  $70^\circ$  shift independent of the pulse delay,  $\tau_d$ . The experimental setup was as described in Fig. 1 ( $U_0 = h \times 5$  kHz). Solid and open circles have the same meaning as in (a). The insets show the time sequence of the optical intensity for the well(s) temporarily turned off.

050405-3

probably too small to be observed. We assume that the measured phase shift can be found by averaging the applied inhomogeneous phase shift over the inhomogeneous condensate density:  $\Delta\bar{\phi} = \frac{1}{N} \int d^3\vec{r} n(\vec{r}) \Delta\phi(\vec{r}) = (U_0 - \frac{2}{7}\mu)\Delta t/\hbar$ , where  $N = \int d^3\vec{r} n(\vec{r})$  is the number of atoms. The measured phase shifts yielded  $U_0 = h \times 5$  kHz [Fig. 4(b)], which was consistent with calculations based on the measured trap frequencies.

The measured phase shifts in the interferometer depended only on the time integral of the applied ac Stark phase shifts [Fig. 4(b)]. For uncoupled condensates, the final relative phase,  $\phi_r$ , should be the same on any phase trajectory because the history of phase accumulation does not affect the total amount of accumulated phase. For coupled condensates, Josephson oscillations between the wells would cause the relative phase to vary nonlinearly with time and produce a time dependent signal in Fig. 4(b). The single-particle tunneling rate and Josephson oscillation frequency in our system were calculated to be  $\sim 5 \times 10^{-4}$  Hz [28] and  $\sim 1$  Hz [31], respectively.

In conclusion, we have performed atom interferometry with Bose-Einstein condensates confined by optical potentials. A coherent condensate beam splitter was demonstrated by deforming a single-well potential into a double-well potential. The large spatial separation between the potential wells allowed each condensate to evolve independently and for addressing each condensate individually. Recombination was performed by releasing the atoms from the double-well potential and allowing them to overlap while expanding ballistically. Implementing a similar readout scheme with magnetic potentials generated by microfabricated current carrying wires should be possible. Propagating the separated condensates along a microfabricated waveguide prior to phase readout would create an atom interferometer with an enclosed area, and hence with rotation sensitivity.

We thank W. Jhe, C.V. Nielsen, and A. Schirotzek for experimental assistance and S. Gupta, Z. Hadzibabic, and M.W. Zwierlein for critical comments on the manuscript. This work was funded by ARO, NSF, ONR, and NASA. M.S. acknowledges additional support from the Swiss National Science Foundation.

\*URL: [http://cua.mit.edu/ketterle\\_group/](http://cua.mit.edu/ketterle_group/)

- [1] A. Peters, K.Y. Chung, B. Young, J. Hensley, and S. Chu, *Philos. Trans. R. Soc. London, Ser. A* **355**, 2223 (1997).
- [2] B.P. Anderson and M.A. Kasevich, *Science* **282**, 1686 (1998).
- [3] A. Lenef, T.D. Hammond, E.T. Smith, M.S. Chapman, R.A. Rubenstein, and D.E. Pritchard, *Phys. Rev. Lett.* **78**, 760 (1997).
- [4] T.L. Gustavson, P. Bouyer, and M.A. Kasevich, *Phys. Rev. Lett.* **78**, 2046 (1997).
- [5] M.S. Chapman, T.D. Hammond, A. Lenef, J. Schmiedmayer, R.A. Rubenstein, E. Smith, and D.E. Pritchard, *Phys. Rev. Lett.* **75**, 3783 (1995).
- [6] C.R. Ekstrom, J. Schmiedmayer, M.S. Chapman, T.D. Hammond, and D.E. Pritchard, *Phys. Rev. A* **51**, 3883 (1995).
- [7] S. Gupta, K. Dieckmann, Z. Hadzibabic, and D.E. Pritchard, *Phys. Rev. Lett.* **89**, 140401 (2002).
- [8] H. Ott, J. Fortagh, G. Schlotterbeck, A. Grossmann, and C. Zimmermann, *Phys. Rev. Lett.* **87**, 230401 (2001).
- [9] W. Hänsel, P. Hommelhoff, T.W. Hänsch, and J. Reichel, *Nature (London)* **413**, 498 (2001).
- [10] A.E. Leanhardt, A.P. Chikkatur, D. Kielpinski, Y. Shin, T.L. Gustavson, W. Ketterle, and D.E. Pritchard, *Phys. Rev. Lett.* **89**, 040401 (2002).
- [11] S. Schneider, A. Kasper, C. vom Hagen, M. Bartenstein, B. Engeser, T. Schumm, I. Bar-Joseph, R. Folman, L. Feenstra, and J. Schmiedmayer, *Phys. Rev. A* **67**, 023612 (2003).
- [12] R. Dumke, T. Mütter, M. Volk, W. Ertmer, and G. Birkl, *Phys. Rev. Lett.* **89**, 220402 (2002).
- [13] E.A. Hinds, C.J. Vale, and M.G. Boshier, *Phys. Rev. Lett.* **86**, 1462 (2001).
- [14] W. Hänsel, J. Reichel, P. Hommelhoff, and T.W. Hänsch, *Phys. Rev. A* **64**, 063607 (2001).
- [15] E. Andersson, T. Calarco, R. Folman, M. Andersson, B. Hessmo, and J. Schmiedmayer, *Phys. Rev. Lett.* **88**, 100401 (2002).
- [16] C. Menotti, J.R. Anglin, J.I. Cirac, and P. Zoller, *Phys. Rev. A* **63**, 023601 (2001).
- [17] J.A. Stickney and A.A. Zozulya, *Phys. Rev. A* **66**, 053601 (2002).
- [18] C. Orzel, A.K. Tuchman, M.L. Fenselau, M. Yasuda, and M.A. Kasevich, *Science* **291**, 2386 (2001).
- [19] F.S. Cataliotti, S. Burger, C. Fort, P. Maddaloni, F. Minardi, A. Trombettoni, A. Smerzi, and M. Inguscio, *Science* **293**, 843 (2001).
- [20] M. Greiner, I. Bloch, O. Mandel, T.W. Hänsch, and T. Esslinger, *Phys. Rev. Lett.* **87**, 160405 (2001).
- [21] M. Greiner, O. Mandel, T. Esslinger, T.W. Hänsch, and I. Bloch, *Nature (London)* **415**, 39 (2002).
- [22] J. Javanainen and M. Wilkens, *Phys. Rev. Lett.* **78**, 4675 (1997).
- [23] A.J. Leggett and F. Sols, *Phys. Rev. Lett.* **81**, 1344 (1998).
- [24] J. Javanainen and M. Wilkens, *Phys. Rev. Lett.* **81**, 1345 (1998).
- [25] M.R. Andrews, C.G. Townsend, H.-J. Miesner, D.S. Durfee, D.M. Kurn, and W. Ketterle, *Science* **275**, 637 (1997).
- [26] O. Mandel, M. Greiner, A. Widera, T. Rom, T.W. Hänsch, and I. Bloch, *Phys. Rev. Lett.* **91**, 010407 (2003).
- [27] T.L. Gustavson, A.P. Chikkatur, A.E. Leanhardt, A. Görlitz, S. Gupta, D.E. Pritchard, and W. Ketterle, *Phys. Rev. Lett.* **88**, 020401 (2002).
- [28] F. Dalfovo, S. Giorgini, L.P. Pitaevskii, and S. Stringari, *Rev. Mod. Phys.* **71**, 463 (1999).
- [29] M. Lewenstein and L. You, *Phys. Rev. Lett.* **77**, 3489 (1996).
- [30] J.A. Dunningham, M.J. Collett, and D.F. Walls, *Phys. Lett. A* **245**, 49 (1998).
- [31] A. Smerzi, S. Fantoni, S. Giovanazzi, and S.R. Shenoy, *Phys. Rev. Lett.* **79**, 4950 (1997).